



Effect of source size and emission time on the p–p momentum correlation function in the two-proton emission process

Long Zhou^{1,2} · De-Qing Fang^{1,3}

Received: 16 February 2020 / Revised: 6 March 2020 / Accepted: 11 March 2020 / Published online: 5 May 2020

© China Science Publishing & Media Ltd. (Science Press), Shanghai Institute of Applied Physics, the Chinese Academy of Sciences, Chinese Nuclear Society and Springer Nature Singapore Pte Ltd. 2020

Abstract The effect of source size and emission time on the proton–proton (p–p) momentum correlation function ($C_{pp}(q)$) has been studied systematically. Assuming a spherical Gaussian source with space and time profile according to the function $S(r, t) \sim \exp(-r^2/2r_0^2 - t/\tau)$ in the correlation function calculation code (CRAB), the results indicate that one $C_{pp}(q)$ distribution corresponds to a unique combination of source size r_0 and emission time τ . Considering the possible nuclear deformation from a spherical nucleus, an ellipsoidal Gaussian source characterized by the deformation parameter $\epsilon = \Delta R/R$ has been simulated. There is almost no difference of $C_{pp}(q)$ between the results of spherically and ellipsoidally shaped sources with small deformation. These results indicate that a unique source size r_0 and emission time could be extracted from the p–p momentum correlation function, which is

especially important for identifying the mechanism of two-proton emission from proton-rich nuclei. Furthermore, considering the possible existence of cluster structures within a nucleus, the double Gaussian source is assumed. The results show that the p–p momentum correlation function for a source with or without cluster structures has large systematical differences with the variance of r_0 and τ . This may provide a possible method for experimentally observing the cluster structures in proton-rich nuclei.

Keywords Two-proton emission · p–p momentum correlation function · Source size · Emission time

1 Introduction

Besides the well-known α , β , and γ radioactivity decays, exotic radioactivity modes also exist in very proton-rich nuclei [1–4]. Two-proton emission is one of the most interesting phenomena in nuclei beyond or close to the proton drip line [5, 6]. Generally speaking, there are three different mechanisms for proton-rich nuclei to emit two protons: (1) two-body sequential emission, (2) three-body simultaneous emission, and (3) diproton emission (also called ^2He cluster emission). The third mode is an extreme case with the emission of two strongly correlated protons. The ^2He cluster can only exist for a short while and then separates after penetrating the Coulomb barrier.

The two-particle momentum correlation is influenced by the nuclear force between two particles [7]; consequently, the proton–proton momentum correlation plays an important role in the emission mechanism and causes the two-proton relative momentum (q_{pp}) and opening angle (θ_{pp}) to be quite different compared with other emission

This work is partially supported by the National Key R&D Program of China (No. 2018YFA0404404), the National Natural Science Foundation of China (Nos. 11925502, 11935001, 11961141003, 11421505, 11475244, and 11927901), the Shanghai Development Foundation for Science and Technology (No. 19ZR1403100), the Strategic Priority Research Program of the CAS (No. XDB34030000), and the Key Research Program of Frontier Sciences of the CAS (No. QYZDJ-SSW-SLH002).

✉ De-Qing Fang
dqfang@fudan.edu.cn

¹ Shanghai Institute of Applied Physics, Chinese Academy of Sciences, Shanghai 201800, China

² University of Chinese Academy of Sciences, Beijing 100049, China

³ Key Laboratory of Nuclear Physics and Ion-beam Application (MOE), Institute of Modern Physics, Fudan University, Shanghai 200433, China

mechanisms [8, 9]. Generally, the two-proton correlation of diproton emission is much stronger than that of the other two mechanisms. Additionally, the emission time difference between two protons for sequential emission is long, compared to the other two modes. In Ref. [10], the three-body decay of two excited proton-rich nuclei, namely $^{23}\text{Al} \rightarrow \text{p} + \text{p} + ^{21}\text{Na}$ and $^{22}\text{Mg} \rightarrow \text{p} + \text{p} + ^{20}\text{Ne}$, has been measured at the RIKEN RI Beam Factory. It has been noted that the emission mechanism of the isospin analogue state (IAS) of ^{22}Mg has strong diproton emission probability, based on the analysis of (q_{pp}) and (θ_{pp}) . However, it is difficult to determine the emission mechanism of the excited ^{23}Al . For three-body simultaneous emission, the two protons are emitted almost at the same time, while the emission time of two-body sequential emission is quite different. Comparing the experimental data with the theoretical simulations, the source size and proton emission time can be extracted [11–13]. In Ref. [14], the p–p momentum correlation function ($C_{pp}(q)$) was studied for these two decay channels, and the source size and emission time information were extracted, as well as for the emission mechanisms of two protons from ^{23}Al and ^{22}Mg .

There are two main factors that affect the p–p momentum correlation function. One is the source size, the other is the emission time difference between the two protons. An increase in the source size will decrease the strength of $C_{pp}(q)$, and the emission time difference will also have a similar effect on $C_{pp}(q)$. However, the source size and emission time determining $C_{pp}(q)$ are unique, or a different combination of source size and emission time could give the same $C_{pp}(q)$. In this study, the p–p momentum correlation function was investigated systematically by using the code Correlation After Burner (CRAB), which is a widely used method for calculating the momentum correlation function in nuclear physics [15]. Assuming the first proton being emitted at time $t = 0$ and the second proton being emitted at time t , a Gaussian source with the form $S(r, t) \sim \exp(-r^2/2r_0^2 - t/\tau)$ is used in CRAB. Here, r_0 refers to the source size and τ refers to the lifetime for the emission time of the second proton [14]. The effect of source size and emission time on $C_{pp}(q)$ was studied systematically. The effect of deformation and different configuration of nuclei was also considered [16, 17].

2 Calculation results

2.1 Spherical Gaussian source

We first calculated the p–p momentum correlation function $C_{pp}(q)$ by assuming a spherical Gaussian source. In Fig. 1, the results of $C_{pp}(q)$ with source size of $r_0 = 0.5$

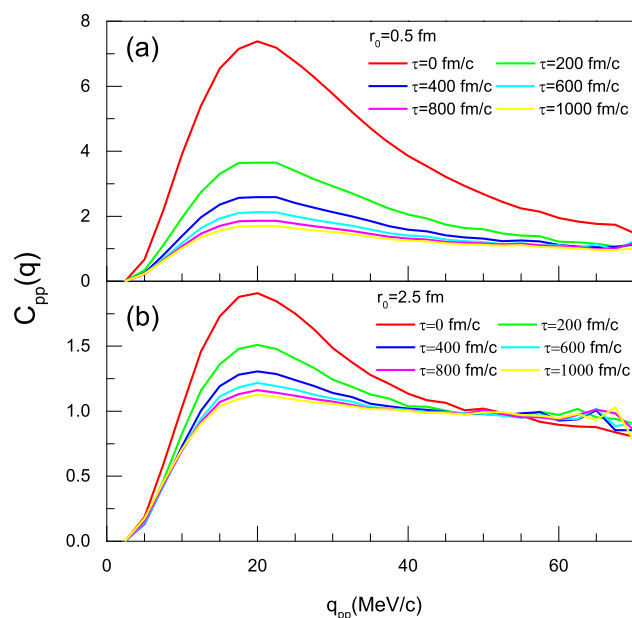


Fig. 1 (Color online) p–p momentum correlation function ($C_{pp}(q)$) for different τ at source size $r_0 = 0.5$ fm (a) and $r_0 = 2.5$ fm (b)

fm and $r_0 = 2.5$ fm at different values of τ are presented. The figure shows that $C_{pp}(q)$ decreases as τ increases for fixed r_0 . For larger r_0 , the difference of $C_{pp}(q)$ between different τ becomes larger.

In Fig. 2, we can see that $C_{pp}(q)$ decreases as r_0 increases for a fixed value of τ . For larger τ , the difference of $C_{pp}(q)$ between different r_0 becomes smaller. In these

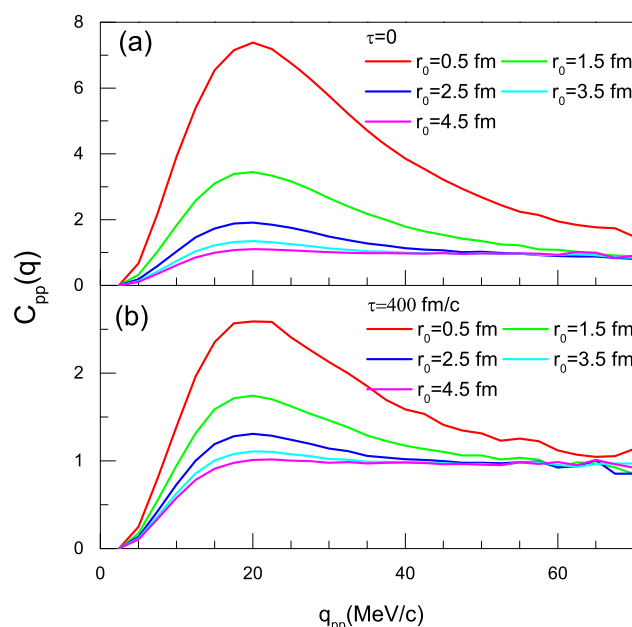


Fig. 2 (Color online) $C_{pp}(q)$ for different r_0 at emission time $\tau = 0$ (a) and $\tau = 400$ fm/c (b)

figures, $C_{pp}(q)$ has the maximum value at around $q_{pp} = 20$ MeV/c.

The proton-proton momentum correlation function $C_{pp}(q)$ increases with q_{pp} and saturates at around 1. Two parameters were used to describe $C_{pp}(q)$ for studying the effect of source size and emission time systematically. One is the maximum value of $C_{pp}(q)$ at approximately $q_{pp} = 20$ MeV/c ($C_{max}(q)$), and the other is the full width at half maximum (FWHM) of $C_{pp}(q)$ determined by the difference of the two q_{pp} values of $C_{pp}(q) = [C_{max}(q) - 1]/2$ located at the left and right side of the $C_{pp}(q)$ maximum. The r_0 dependence of $C_{max}(q)$ and FWHM for the p-p momentum correlation function with different τ are given in Fig. 3. As shown in Fig. 3a, $C_{max}(q)$ decreases gradually with increasing r_0 . For a large τ , the change of $C_{max}(q)$ is very small. As shown in Fig. 3b, the FWHM is inversely proportional to r_0 . For different τ , the behavior of the FWHM with r_0 is very similar.

Similarly, the τ dependence of $C_{max}(q)$ and the FWHM for the p-p momentum correlation function at different r_0 are shown in Fig. 4. The dependence of $C_{max}(q)$ on τ is quite similar with r_0 , except for the FWHM results. The difference of the FWHM values is much larger for different source sizes.

Since both r_0 and τ affect the correlation function, it is interesting to see whether or not different r_0 and τ combinations result in the same proton-proton momentum correlation function $C_{pp}(q)$. To find the answer, contour plots of $C_{max}(q)$ and the FWHM extracted from $C_{pp}(q)$ at different r_0 and τ values are given in Fig. 5, in which

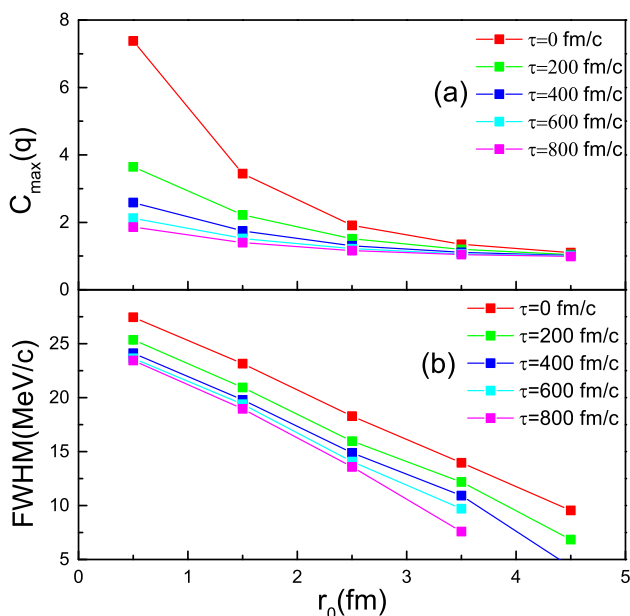


Fig. 3 (Color online) The r_0 dependence of $C_{max}(q)$ (a) and the FWHM (b) for the p-p momentum correlation function at different τ

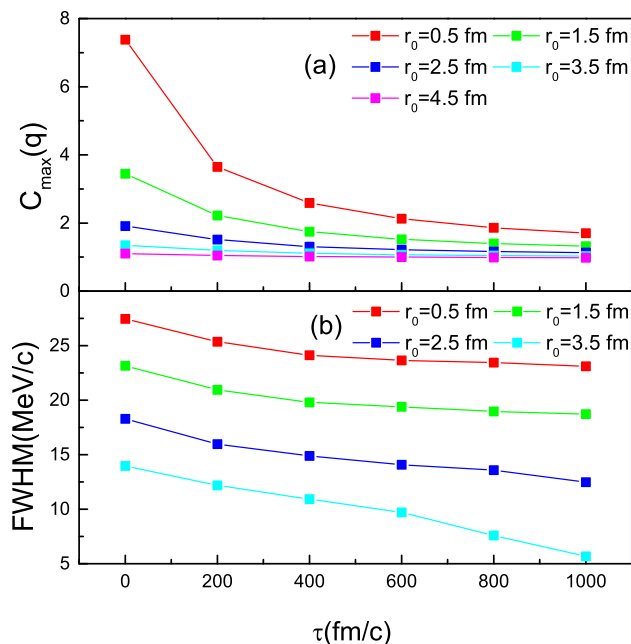


Fig. 4 (Color online) τ dependence of $C_{max}(q)$ (a) and the FWHM (b) for the p-p momentum correlation function at different r_0

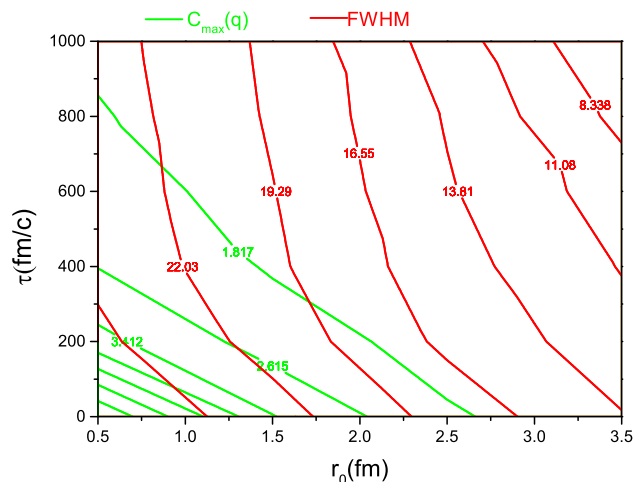


Fig. 5 (Color online) Contour plot of $C_{max}(q)$ and the FWHM extracted from the p-p momentum correlation function

$C_{max}(q)$ and the FWHM are the Z axis. From this figure, we can see clearly that each isoline of $C_{max}(q)$ or the FWHM has only one intersection point with each other. This indicates that a set of $C_{max}(q)$ and the FWHM values or one proton-proton momentum correlation function has only a uniquely determined r_0 and τ combination. This is due mainly to the monotonic dependence of $C_{max}(q)$ or the FWHM on r_0 and τ , respectively. Based on the above results, it is shown that the source size r_0 and proton emission time difference τ could be determined uniquely by fitting the experimental $C_{pp}(q)$ with the CRAB calculation, as demonstrated in [14].

2.2 Ellipsoidal Gaussian source

Considering the possible deformation of the nucleus, we calculated the proton–proton correlation function $C_{pp}(q)$ for a deformed nucleus through the CRAB code. The deformation is described by the parameter $\epsilon = \Delta R/R$, where R is the nuclear radius with no deformation and ΔR is the difference in radius before and after the deformation.

After considering the deformation of the source using CRAB, the calculated $C_{pp}(q)$ results are shown in Fig. 6. The $C_{\max}(q)$ and the FWHM of the ellipsoidal Gaussian source and the spherical Gaussian source are almost same in the range of ϵ from -0.10 to 0.10 . In fact, the $C_{pp}(q)$ of the ellipsoidal Gaussian source and the spherical Gaussian source are almost identical, with the same effective source radius r_0 . This indicates that the deformation (not very large) of the nucleus has little effect on the p–p momentum correlation function.

2.3 Double Gaussian source

The α cluster structure is one of the most common aspects of a nucleus [18]. If two protons are emitted from this kind of nucleus, the protons may come from the same or different α cluster within it. It would be interesting to see the effect of the α cluster on the p–p momentum correlation function. To study the cluster structure in the nucleus, a double Gaussian source was used in CRAB to simulate two clusters inside the nucleus.

We assume that the source of two protons is not distinguished. Thus, the two emitted protons may come from

the same cluster or from two different clusters. Define $\Delta C_{\max}(q)$ and ΔFWHM as the difference of $C_{\max}(q)$ and FWHM between the spherical Gaussian source and the double Gaussian source with the same effective source size r_0 . The results of $\Delta C_{\max}(q)$ and ΔFWHM are presented in Fig. 7. In Fig. 7a, $\Delta C_{\max}(q)$ first increases and then decreases with r_0 , and the maximum value appears near $r_0 = 1.5$ fm, i.e., the p–p momentum correlation function has the largest difference for two protons emitted from ordinary nuclei and from nuclei with clusters. $\Delta C_{\max}(q)$ has the largest value when the source size is near 1.5 fm. As shown in Fig. 7b, $\Delta C_{\max}(q)$ decreases as τ increases. For different r_0 , the $\Delta C_{\max}(q)$ values are very large when τ is small, but they are quite close when τ is large enough. We can also see that ΔFWHM gradually increases with r_0 , but there is almost no change with the increase in τ , as shown in Fig. 7c, d.

$\Delta C_{\max}(q)$ decreases with increasing τ , while ΔFWHM does not change with τ , which indicates that the difference of $C_{pp}(q)$ between the double Gaussian source and the spherical Gaussian source decreases and nears the same value with increasing τ . $\Delta C_{\max}(q)$ decreases with increasing r_0 , while ΔFWHM gradually increases with r_0 , which indicates that the difference of $C_{pp}(q)$ between the double Gaussian source and the spherical Gaussian source becomes significantly larger as r_0 increases. These results indicate that the p–p momentum correlation function for a source with or without cluster structure will have large systematical differences with the variance of r_0 and τ . This may provide a possible method for experimentally

Fig. 6 (Color online) Deformation parameter, ϵ , dependence on $C_{\max}(q)$ for different τ at $r_0 = 2.5$ fm (a) and for different r_0 at $\tau = 400$ fm/c (b); the same dependence of the FWHM for different τ at $r_0 = 2.5$ fm (c) and for different r_0 at $\tau = 400$ fm/c (d)

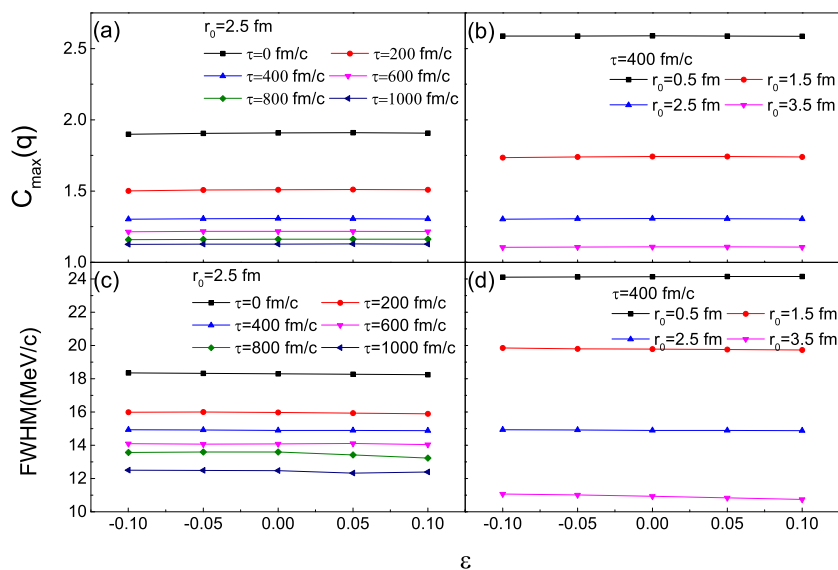
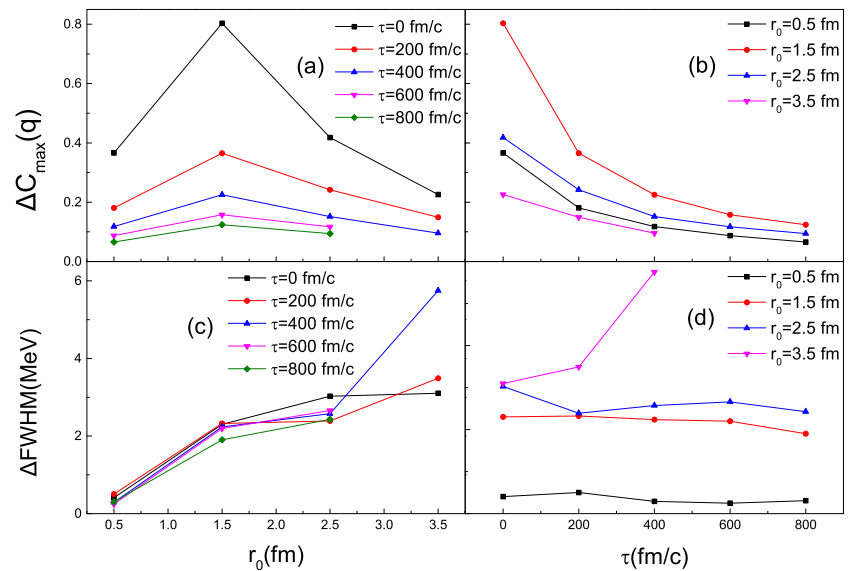


Fig. 7 (Color online) Differences of $C_{\max}(q)$ ($\Delta C_{\max}(q)$) between a spherical Gaussian source and a double Gaussian source for different τ (a) and r_0 (b); the differences of the FWHM (ΔFWHM) between a spherical Gaussian source and a double Gaussian source for different τ (c) and r_0 (d)



observing the cluster structure in proton-rich nuclei. For practical applications, further investigations are necessary.

3 Summary and outlook

In summary, the proton–proton momentum correlation functions ($C_{pp}(q)$) for a sphere, ellipsoid, and double Gaussian source were investigated using the CRAB code. From systematical studies of the varied effects of the source size r_0 and emission time τ on $C_{pp}(q)$, it was shown that one $C_{pp}(q)$ distribution corresponds to unique values of r_0 and τ . There is almost no difference in $C_{pp}(q)$ between a spherical Gaussian source and an ellipsoidal Gaussian source, i.e., a small nuclear deformation has very little effect on $C_{pp}(q)$. The proton–proton momentum correlation function has the largest difference between ordinary nuclei and clustered nuclei when the source size is near 1.5 fm; this may give a possible method for experimentally observing the cluster structure of proton-rich nuclei. Recently, artificial neural networks have been widely used in the research of many practical problems that are difficult for modern computers to solve [19–22]. Extracting the source size and emission time of two particles from experimental data is relatively difficult. It may be interesting to study systematically the p–p momentum correlation functions by using artificial neural networks in future studies.

References

1. M. Pfutzner, M. Karny, L.V. Grigorenko et al., Radioactive decays at limits of nuclear stability. *Rev. Mod. Phys.* **84**, 567 (2012). <https://doi.org/10.1103/RevModPhys.84.567>
2. B. Blank, M. Ploszajczak, Two-proton radioactivity. *Rep. Prog. Phys.* **71**, 046301 (2008). <https://doi.org/10.1088/0034-4885/71/4/046301>
3. E. Olsen, M. Pfutzner, N. Birge et al., Landscape of two-proton radioactivity. *Phys. Rev. Lett.* **110**, 222501 (2013). <https://doi.org/10.1103/PhysRevLett.110.222501>
4. K.W. Brown, R.J. Charity, L.G. Sobotka et al., Observation of long-range three-body Coulomb effects in the decay of ^{16}Ne . *Phys. Rev. Lett.* **113**, 232501 (2014). <https://doi.org/10.1103/PhysRevLett.113.232501>
5. V.I. Goldansky, On neutron-deficient isotopes of light nuclei and the phenomena of proton and two-proton radioactivity. *Nucl. Phys.* **19**, 482 (1960). [https://doi.org/10.1016/0029-5582\(60\)90258-3](https://doi.org/10.1016/0029-5582(60)90258-3)
6. Y.T. Wang, D.Q. Fang, X.X. Xu et al., Implantation-decay method to study the β -delayed charged particle decay. *Nucl. Sci. Tech.* **29**, 98 (2018). <https://doi.org/10.1007/s41365-018-0438-5>
7. Z.Q. Zhang, Y.G. Ma, Measurements of momentum correlation and interaction parameters between antiprotons. *Nucl. Sci. Tech.* **27**, 152 (2016). <https://doi.org/10.1007/s41365-016-0147-x>
8. R.A. Kryger, A. Azhari, M. Hellstrom et al., Two-proton emission from the ground state of ^{12}O . *Phys. Rev. Lett.* **74**, 860 (1995). <https://doi.org/10.1103/PhysRevLett.74.860>
9. G. Raciti, G. Cardella, M. De Napoli et al., Experimental evidence of ^2He decay from ^{18}Ne excited states. *Phys. Rev. Lett.* **100**, 192503 (2008). <https://doi.org/10.1103/PhysRevLett.100.192503>
10. Y.G. Ma, D.Q. Fang, X.Y. Sun et al., Different mechanism of two-proton emission from proton-rich nuclei ^{23}Al and ^{22}Mg . *Phys. Lett. B* **743**, 306 (2015). <https://doi.org/10.1016/j.physletb.2015.02.066>
11. M.A. Lisa, C.K. Gelbke, P. Decowski et al., Observation of lifetime effects in two-proton correlations for well-characterized sources. *Phys. Rev. Lett.* **71**, 2863 (1993). <https://doi.org/10.1103/PhysRevLett.71.2863>

12. G. Verde, A. Chbihi, R. Ghetti et al., Correlations and characterization of emitting sources. *Eur. Phys. J. A* **30**, 81 (2006). <https://doi.org/10.1140/epja/i2006-10109-6>
13. W.A. Zajc, J.A. Bistirlich, R.R. Bossingham et al., Two-pion correlations in heavy ion collisions. *Phys. Rev. C* **29**, 2173 (1984). <https://doi.org/10.1103/PhysRevC.29.2173>
14. D.Q. Fang, Y.G. Ma, X.Y. Sun et al., Proton–proton correlations in distinguishing the two-proton emission mechanism of ^{23}Al and ^{22}Mg . *Phys. Rev. C* **94**, 044621 (2016). <https://doi.org/10.1103/PhysRevC.94.044621>
15. S. Pratt, J. Sullivan, H. Sorge et al., Testing transport theories with correlation measurements. *Nucl. Phys. A* **566**, 103c (1994). [https://doi.org/10.1016/0375-9474\(94\)90614-9](https://doi.org/10.1016/0375-9474(94)90614-9)
16. M. Aygun, Z. Aygun, A theoretical study on different cluster configurations of the ^9Be nucleus by using a simple cluster model. *Nucl. Sci. Tech.* **28**, 86 (2017). <https://doi.org/10.1007/s41365-017-0239-2>
17. C. Constantinou, M.A. Caprio, J.P. Vary et al., Natural orbital description of the halo nucleus ^6He . *Nucl. Sci. Tech.* **28**, 179 (2017). <https://doi.org/10.1007/s41365-017-0332-6>
18. W. von Oertzen, M. Freer, Y. Kanada-En'yo, Nuclear clusters and nuclear molecules. *Phys. Rep.* **432**, 43 (2006). <https://doi.org/10.1016/j.physrep.2006.07.001>
19. Y. Liu, J.J. Zhu, N. Roberts et al., Recovery of saturated signal waveform acquired from high-energy particles with artificial neural networks. *Nucl. Sci. Tech.* **30**, 148 (2019). <https://doi.org/10.1007/s41365-019-0677-0>
20. H.K. Yang, K.C. Liang, K.J. Kang et al., Slice-wise reconstruction for low-dose cone-beam CT using a deep residual convolutional neural network. *Nucl. Sci. Tech.* **30**, 59 (2019). <https://doi.org/10.1007/s41365-019-0581-7>
21. H.L. Zheng, X.G. Tuo, S.M. Peng et al., Determination of Gamma point source efficiency based on a back-propagation neural network. *Nucl. Sci. Tech.* **29**, 61 (2018). <https://doi.org/10.1007/s41365-018-0410-4>
22. A. Gheziel, S. Hanini, B. Mohamedi et al., Particle dispersion modeling in ventilated room using artificial neural network. *Nucl. Sci. Tech.* **28**, 5 (2017). <https://doi.org/10.1007/s41365-016-0159-6>